Component III Lab Report

Shane Kalani Abbley

Abstract:

Our F182Y urate oxidase was successfully mutated, expressed, and purified at the start of this experiment. We ran a spectrophotometric kinetics experiment to try to understand how our mutation affected the protein. This experiment measured the disappearance of the substrate over time. From this we obtained results that indicate decreased activity of the mutant enzyme relative to the wild type enzyme. We used this data and the visualization of the molecules to try to understand how the mutation affected the structure and function of the enzyme.

Introduction:

This is the final component of our experiment analyzing our mutant F182Y variant of the *Bacillus subtilis* urate oxidase isoform. Up to this point, we have successfully performed site directed mutagenesis on a cloning vector, transformed that vector into host competent cells, and multiplied, harvested, and purified the plasmid in component I. In component II, we transformed this plasmid into an expression competent cell, overexpressed and harvested the protein, and purified the protein to a respectable specific activity. Now we are ready to determine how our mutation affected the protein's kinetics and structure.

Kinetics Measurements and Calculations:

The objective of this component is to attempt to characterize our F182Y mutation. This can be determined from the values of the Michaelis Menten constant (K_m) and the turnover number (k_{cat}). That is, if the k_{cat} significantly decreases, but the K_m does not change, then one can reasonably assume that the residue is involved in the chemical step of the enzyme-substrate complex (ES) or in transition-state (TS) stabilization. This is because the release of substrate has a higher ratio of reverse/forward rate constant. If k_{cat} is increasing, then one can likely conclude that the residue is important in the release step. If only K_m changes, it is likely that the residue is directly involved in substrate binding. We know our residue is likely involved in the stabilization of the transition state because it stacks against a phenylalanine which stacks directly with the aromatic ring of urate, so we expect to see a decreasing k_{cat}. For our specific mutation, we may also be able to test the affinity for alternative substrates. The increased bulkiness of the hydroxyl group may result in significantly decreased activity for larger substrates compared to smaller ones. That being said, because our mutation is somewhat removed from the active site, this may not contribute significantly.

We are taking measurements at 292 nm to measure the disappearance of urate in our solution. We can not measure the appearance of allantoin because there is an intermediate 5-hydroxyisourate formation step. 5-hydroxyisourate also absorbs at 292 nm; however, we are performing the reaction at a pH of 9.15 and 5-hydroxyisourate is not particularly stable at this pH. The rate calculation time is set to 70 seconds so that enough data is collected for the calculation of the rate. If too little data is present we will get inaccurate results due to random error. If we measure

for too long, we would be wasting our time because we are primarily interested in the initial velocity. We will use these initial velocities and the substrate concentrations in order to perform a nonlinear regression using the Michaelis-Menten kinetics model. This will inform us of our values of V_{max} and K_M. V_{max} is determined from the horizontal asymptote of the graph and the K_M is equal to the substrate concentration value where $V = V_{max}$.
The only independent variable is the concentration of urate so the CHES buffer is still in use to reduce fluctuations in pH and to maintain the stability of our enzyme. Similarly, the quartz cuvette, CHES and urate are kept warm so that our cold enzyme does not change the temperature of the solution significantly. Our enzyme will function better at these higher temperatures, despite the fact that it will destabilize much quicker. Of course, all of this is only relevant when compared to the wild type enzyme, so we will measure the same data for the wild type in order to compare kinetics data.

Molecular Visualization:
Molecular visualization allows for computer based modeling of molecular structures This is useful in biochemistry, materials science, biology and many other fields to further develop an understanding of how the structure results in the properties of interest. After this, one could also predict how alterations in structure would affect specific functions of the molecule of interest.

For our purposes, spatial properties of urate oxidase were measured, recorded, and then shared via a PDB file. This PDB file will help us analyze the active site of urate oxidase. We will load the PDB file into Pymol, a molecular visualization program, to see the residues that interact with the active site. We will particularly focus on the mutation that we have created, F182Y, and how the native phenylalanine reacts with surrounding amino acids. In particular, we will be analyzing the 1J2G PDB file. The zoomed in residue shots below were obtained from the 1R51 residue. We will show the native sequence and then the predicted structure from the mutated sequence.
We will utilize Pymol because it has a user friendly interface and we already have significant experience with using it. Pymol has all the functionality that we would desire in analyzing our protein, including: distance measurements, hydrogen bonding, relative spatial positions, and overall protein superstructures. We will use Pymol to compare the mutant to the wild type enzyme.

Methods:

We set the water circulator to 25 ℃ and the spectrophotometer to single wavelength, single cell kinetics with detection at 292 nm. We also set the data collection to 70 s intervals, the rate calculation time to 60 s, and the lag time to 10 s. In a cm quartz cuvette we added 1 mL of CHES buffer and ran a baseline correction. We prepared the 11 samples in figure 1 of varying urate concentrations. We let the cuvettes warm up for 2 minutes in the spectrophotometer prior to running each sample. Next, we added the appropriate volumes of warm CHES buffer and urate

solutions from the table and then added 20 µL of cold enzyme solution to the cuvettes. We covered and gently inverted the cuvette to mix the solutions. We ran all samples in the spectrophotometer and recorded their initial absorbances and the observed rates.

Sample Number	[urate] (µM)	Volume of urate solution (µL)	Volume of CHES (µL)
1	175	875	105
2	150	750	230
3	120	600	380
4	100	500	480
5	80	400	580
6	60	300	680
7	40	200	780
8	30	150	830
9	20	100	880
10	10	50	930
11	5	25	955

Figure 1: Concentrations and volumes of prepared samples for determining the initial absorbances and observed rates of our F182Y mutation.

Results:

The enzyme concentration for urate oxidase was determined from the absorbance at 280 nm, the known molar extinction coefficient, and their relationship in Beer's Law to be 106 µM. 20 µL of enzyme solution was used in each mutant sample. For the wild-type samples 16 µL of 9 µM enzyme stock solution was used in the samples. The k_{cat} was determined by dividing the V_{max} by the concentration of the enzyme. Using a 5% error of concentration, the mutant k_{cat} values range from 1.73495 to 1.91758s^{-1}. Using a 5% error of concentration, the wild-type k_{cat} values range from 15.619 to 17.2632 s^{-1}.

Sample Number	Initial Absorbance	Observed Rate (AU/min)
1	2.14600	0.148
2	1.83320	0.151
3	1.45470	0.162
4	1.19000	0.146
5	0.97090	0.135
6	0.72940	0.118
7	0.47290	0.101
8	0.36520	0.084
9	0.23780	0.068
10	0.11980	0.040
11	0.05450	0.020

Figure 2: Table of mutant kinetic parameters.
The observed rates were calculated from the linear regression of the absorbance vs time data

Sample Number	[urate] (μM)	Initial Absorbance	Observed Rate (AU/min)
1	5	0.06210	0.018
2	10	0.11460	0.037
3	20	0.22170	0.065
4	30	0.34390	0.080
5	40	0.42980	0.092
6	60	0.72460	0.109
7	80	0.97400	0.120
8	100	1.17900	0.115
9	120	1.43400	0.115
10	140	1.69630	0.122

Figure 3: Table of wild-type kinetic parameters.
This was a table of the provided wild-type enzyme kinetic parameters.

Mutant kcat (s^{-1})	Mutant Km (M)	Mutant Vmax (AU/min)	Wild-Type kcat (s^{-1})	Wild-Type Km (M)	Wild-Type Vmax (AU/min)
1.8217	36.68	0.1931	16.4	25.70	0.1476

Figure 4: Table of derived kinetic variables

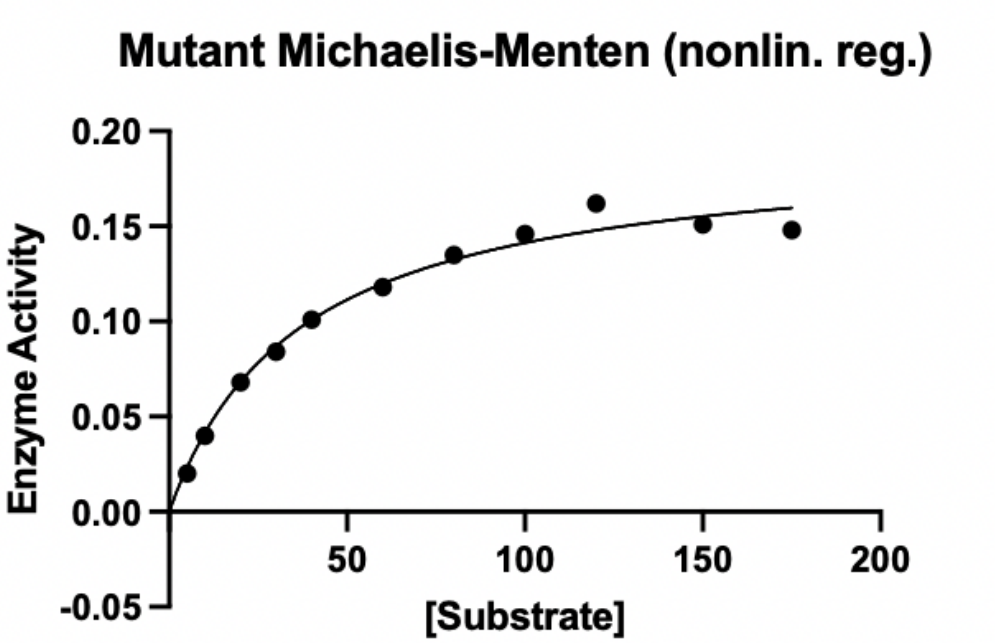

Figure 5: Michaelis Menten fit of our mutant enzyme initial velocities vs substrate concentration. This fit has an R squared value of 0.9826, 9 degrees of freedom, and a sum of squares equal to 0.0004045. The 95% confidence interval gives a range of 0.1767 to 0.2128 AU/min for our V_{max} and 27.77 to 48.49 M for our K_m.

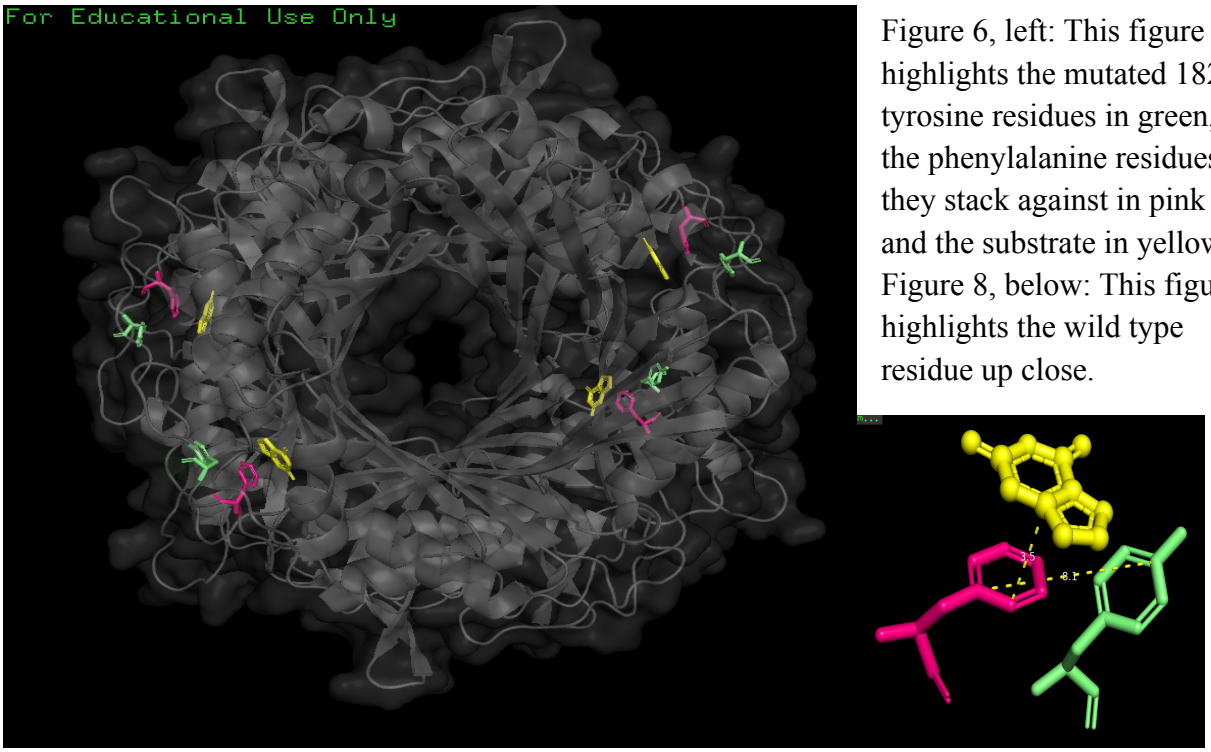

Figure 6, left: This figure highlights the mutated 182 tyrosine residues in green, the phenylalanine residues they stack against in pink and the substrate in yellow.
Figure 8, below: This figure highlights the wild type residue up close.

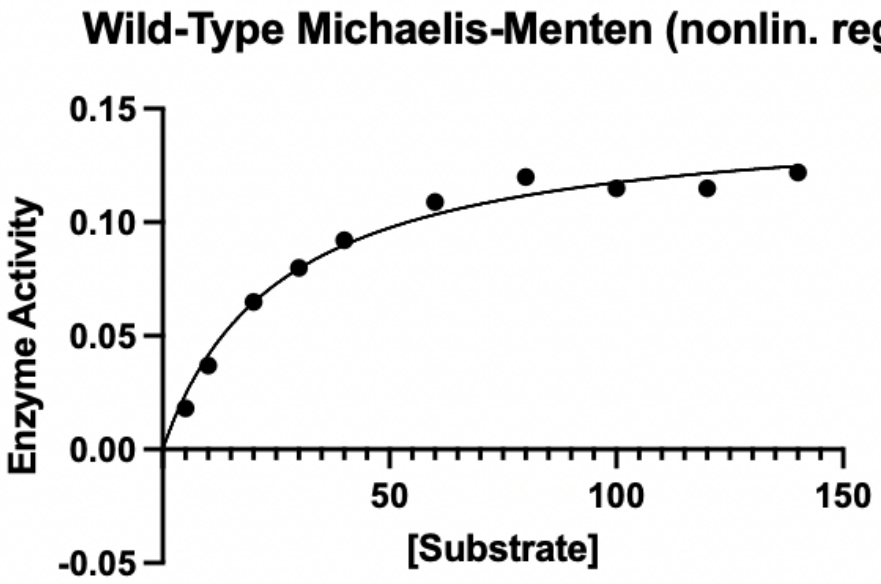

Figure 7: Michaelis Menten fit of our wild-type enzyme initial velocities vs substrate concentrations. This fit has an R squared value of 0.9822, 8 degrees of freedom, and a sum of squares of 0.0002174. The 95% confidence interval gives a range of 0.1357 to 0.1617 AU/min for our V_{max} and 19.37 to 34.06 M for our K_m.

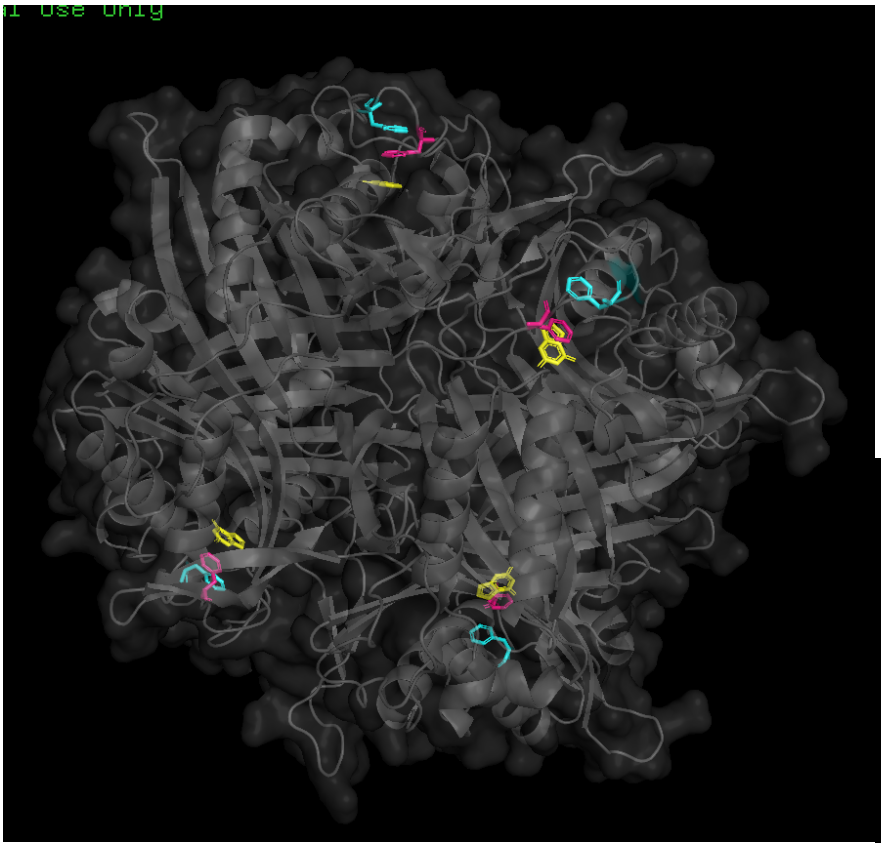

Figure 8, left: This figure highlights the wild type 182 phenylalanine residues in blue, the phenylalanine residues they stack against in pink and the substrate in yellow.

Figure 8, below: This figure highlights the wild type residue up close.

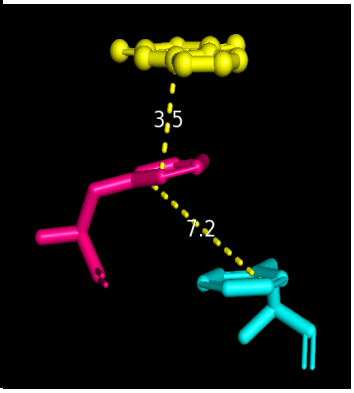

Discussion:

Our mutant urate oxidase showed comparable initial velocities to that of the wild type enzyme. The initial velocities are derived from the linear regressions of the absorbance vs time data points. The initial absorbance values are primarily a function of the concentration of the urate and thus do not tell us much about the presence and or function of our enzyme. The K_m value of the mutant enzyme is surprisingly high. This typically means that the enzyme has a fairly low affinity for the substrate. This explains why significantly higher mutant enzyme concentrations are required to achieve the same initial rates as the wild-type. Furthermore, our k_{cat} for the mutant enzyme is significantly lower than the wild type. This was also predicted by our zoomed in photos of the active site. Specifically, the distance between the phenylalanine that stabilizes the substrate and the mutated tyrosine is greater than that of the wild-type tyrosine. The mutation altered the K_{cat} significantly more than it affected the K_m. This implies that the mutated residue stabilizes the transition state. This makes logical sense because the ring stacking interaction is greater in the wild-type residue than in the mutant. The main source of error in this experiment would derive from the purification of the enzyme rather than in the kinetics experiment. This is because the kinetics experiment was fairly straightforward and only had one main section where human error could be significant. In the protein purification process, we performed 8 days of experiments. Despite our protein solution containing 106 μM enzyme, it is likely that significantly less than this is active. This is because we determined the concentration of the enzyme based on its absorbance at 280 rather than by a method that would differentiate between active and inactive enzyme. Something like an additional activity based assay prior to this final measurement would have helped in this regard.

Conclusions:

Our mutated urate oxidase enzyme showed activity despite the lesser stability provided by the new residue. We learned that the enzyme is most likely involved in stabilizing the transition state. This was predicted because of the nature of the interaction between the active site residues and the substrate. From the beginning of this urate oxidase experiment our primary objective was to see how the mutation would affect the activity of the enzyme. We have deduced this empirically and used molecular visualization to help explain the interactions that create this discrepancy.

References:

1) Khan, K; Parsons, S; Kohn, J. Theory Manual: Laboratory Techniques in Biochemistry. Department of Chemistry and Biochemistry University of California, Santa Barbara (2021), 118-124.

2) Khan, K. Biochemistry Laboratory Operation Manual (CHEM 125L): The Operations Manual for Component III. Department of Chemistry and Biochemistry University of California, Santa Barbara (2021), 1-12.

Appendix:

Linear Fitting over Full Span:

Sample 1:

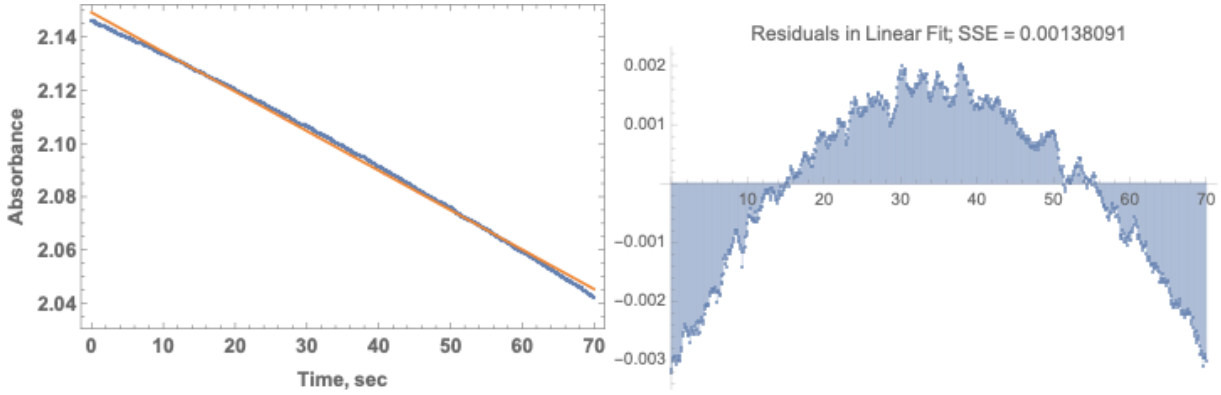

Fitted Model: y = 2.14922 - 0.00148427x

Sample 2:

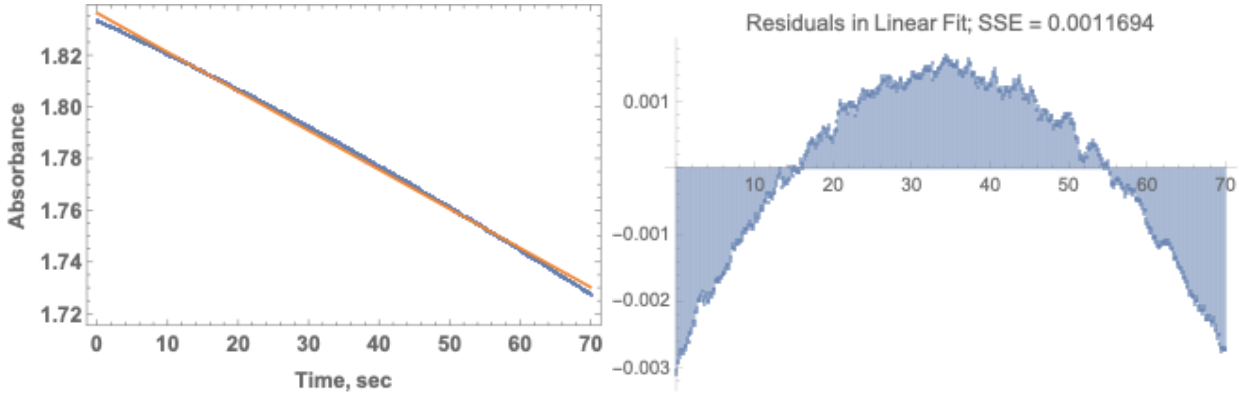

Fitted Model: y = 1.83624 - 0.00151436x

Sample 3:

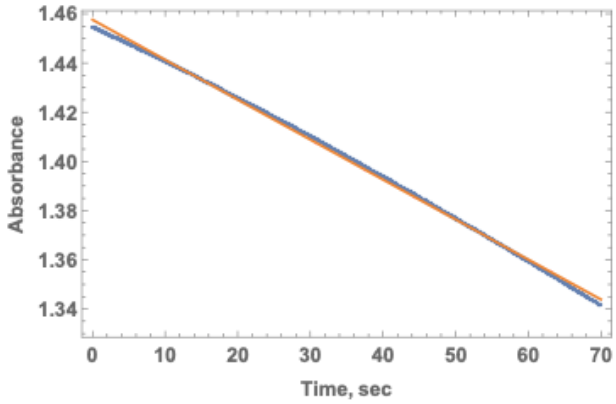

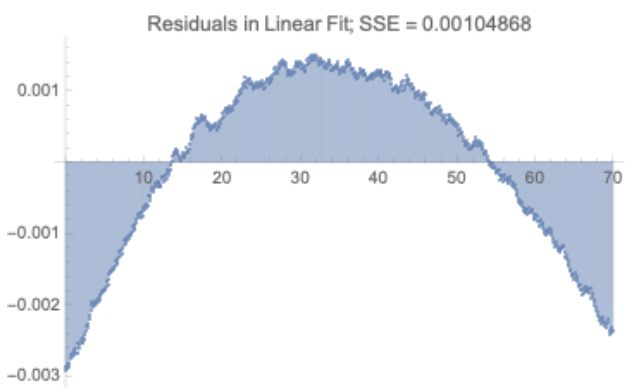

Fitted Model: y = 1.45758 - 0.00162453x

Sample 4:

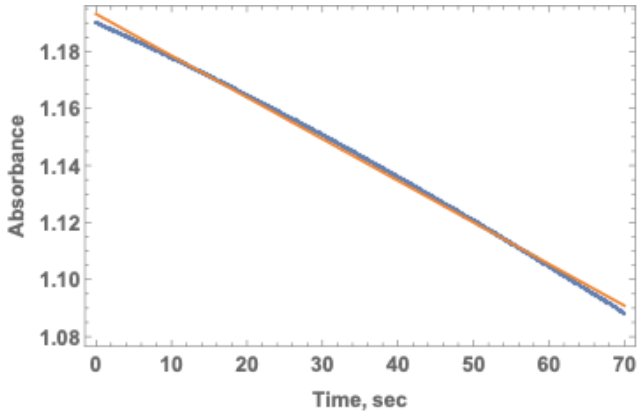

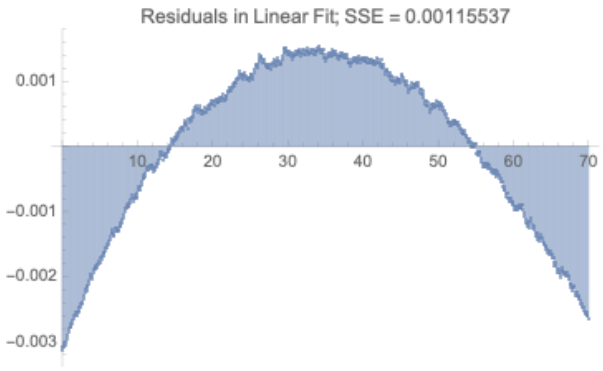

Fitted Model: y = 1.19313 - 0.00146107x

Sample 5:

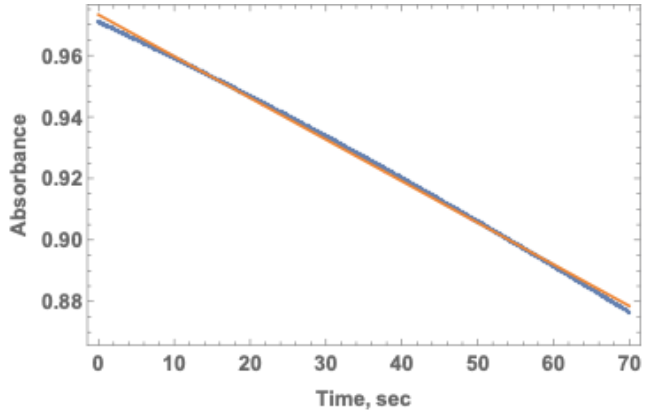

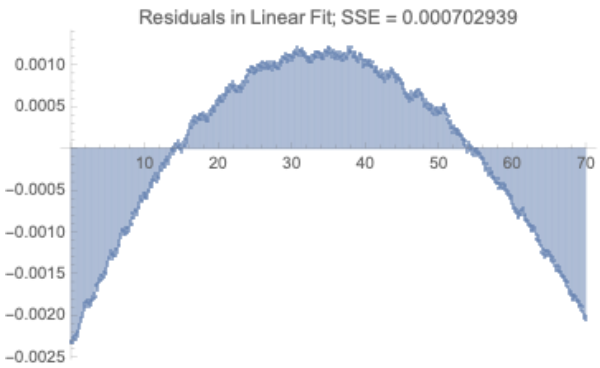

Fitted Model: y = 0.973234 - 0.00135306x

Sample 6:

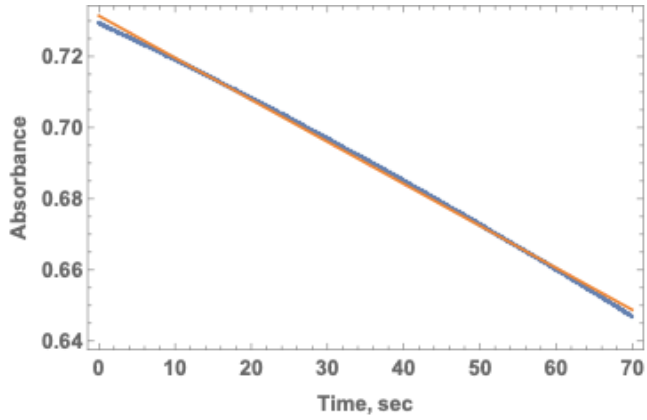

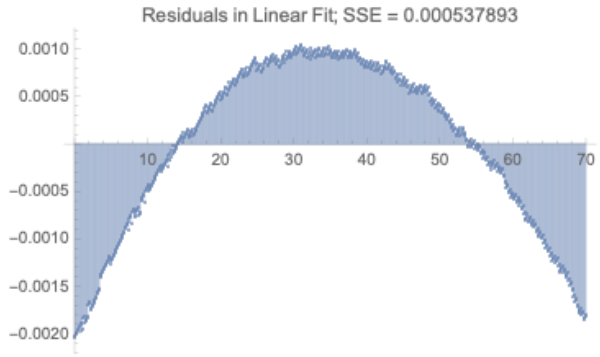

Fitted Model: y = 0.731446 - 0.00118067x

Sample 7:

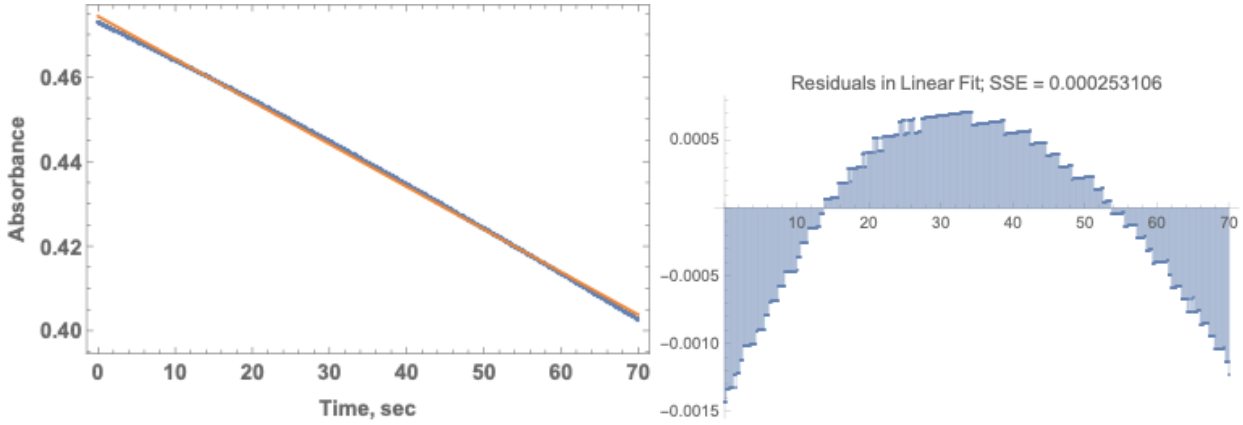

Fitted Model: y = 4.74335 - 0.00100724x

Sample 8:

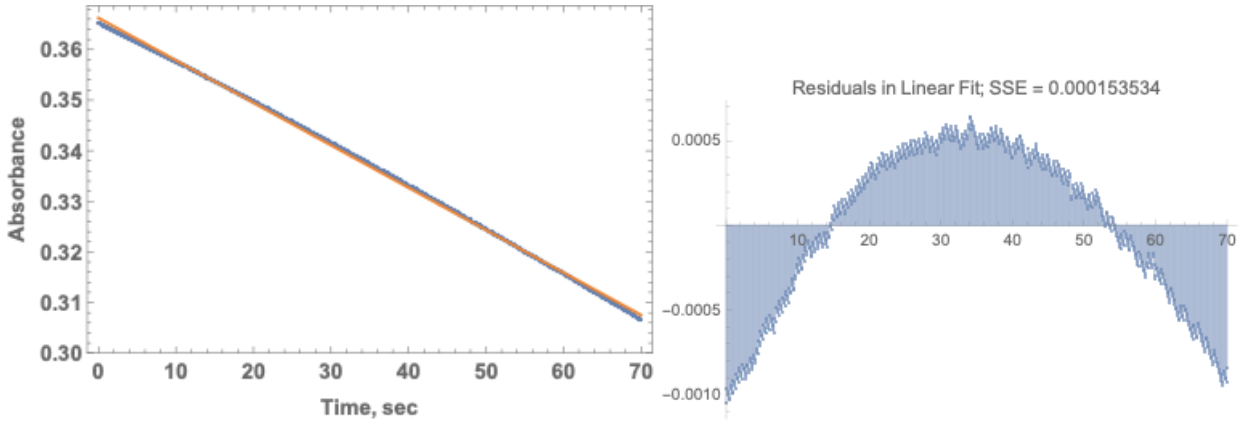

Fitted Model: y = 3.66253 - 0.000838689x

Sample 9:

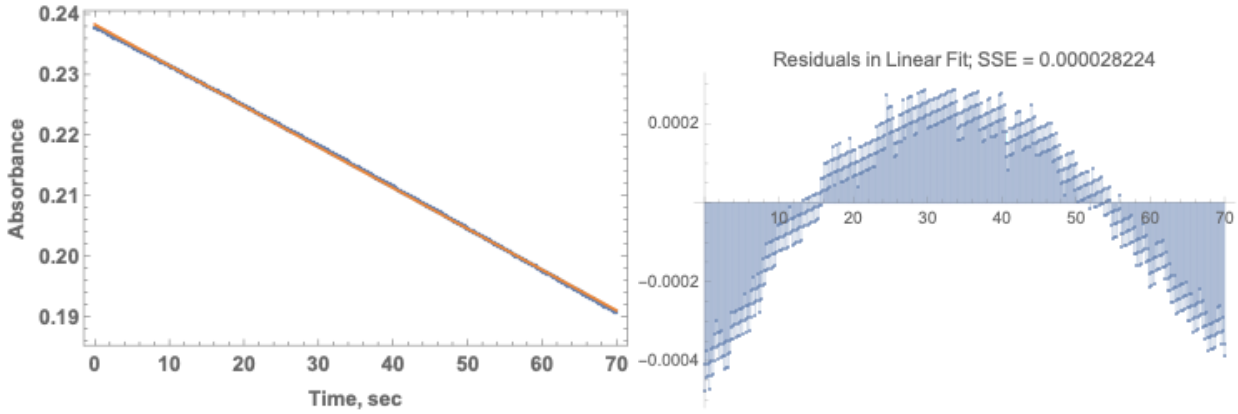

Fitted Model: y = 0.238278 - 0.000675557x

Sample 10:

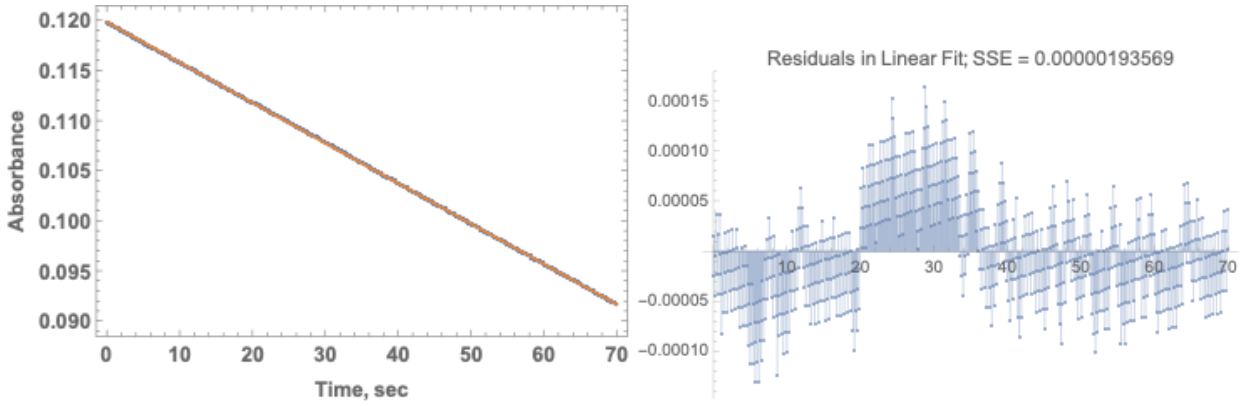

Fitted Model: y = 0.119825 - 0.000402374x

Sample 11:

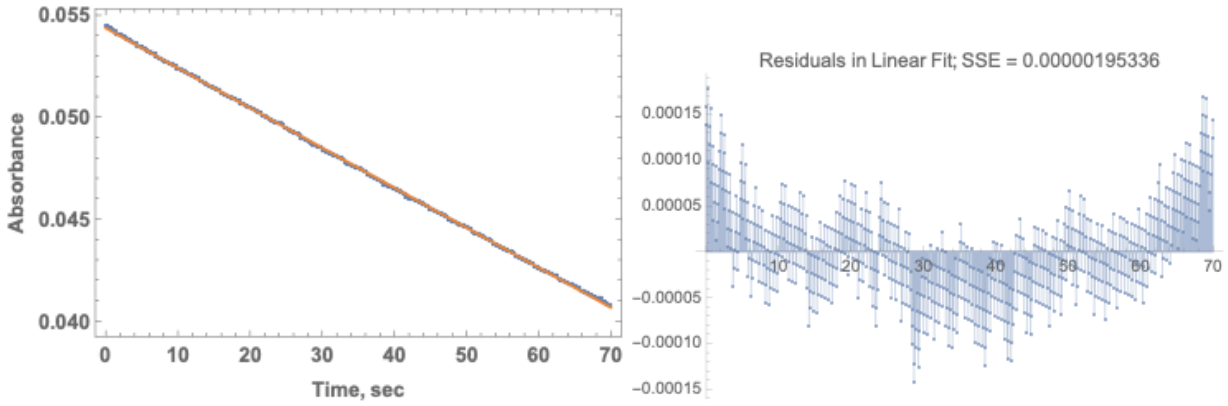

Fitted Model: y = 0.054362 - 0.000195788x